Journal of the Korean Magnetic Resonance Society **2012**, *16,* 162-171

Backbone ^{1}H, ^{15}N, and ^{13}C resonance assignments and secondary structure prediction of SAV2228 (translation initiation factor-1) from *Staphylococcus aureus*

Do-Hee Kim, Sun-Bok Jang and Bong-Jin Lee*

Research Institute of Pharmaceutical Sciences, College of Pharmacy, Seoul National University, Gwanak-Ro 1 , Gwanak-Gu, Seoul 151-742, Korea
(Received Nov 9, 2012; Revised Nov 30, 2012; Accepted Dec 10, 2012)

Abstract : SAV2228 has an OB (Oligomer-Binding)-motif which is frequently used for nucleic acid recognition. To characterize the activity of translation initiation factor-1 (IF-1) from *Staphylococcus aureus,* SAV2228 was expressed and purified in *Escherichia coli*. We acquired 3D NMR spectra showing well dispersed and homogeneous signals which allow us to assign 94.4% of all ^{1}HN, ^{15}N, $^{13}C\alpha$, $^{13}C\beta$ and ^{13}CO resonances.

We could predict a secondary structure of SAV2228 using TALOS and CSI from NMR data. SAV2228 was consisted of one α-helix and five β-sheets. The predicted secondary structure, β-β-β-α-β-β, was similar to other bacterial IF-1, but it was not completely same to the eukaryotic one. Assigned NMR peaks and secondary structre prediction can be used for the study on interaction with nucleic acid in the future.

Keywords : SAV2228, NMR, *Staphylococcus aureus*, OB-motif, IF1

INTRODUCTION

Problem of antibiotic resistance has been increased because patients used antibiotics too much for a long time and the environment inside hospitals makes it worse. The 30 to 50 percents of patients

Research Institute of Pharmaceutical Sciences, College of Pharmacy, Seoul National University, Seoul 151-742, Republic of Korea
email: lbj@nmr.snu.ac.kr
Journal of the Korean Magnetic Resonance Society 2012 December; 16(2): 162-171
http://dx.doi.org/10.6564/JKMRS.2012.16.2.162

have at least one kind of antibiotics resistance[1,2]. Therefore, it is the issue for pharmaceutists to overcome.

Staphylococcus aureus (*S.aureus*) exists as the normal flora in human skin, laryngopharynx, and so on. It is a major opportunistic infections bacterium that causes a life-threatening illness such as the mild inflammation, sepsis, meningitis, and toxic shock syndrome. If the infection of *S.aureus* is occurred in the wounds of patients with reduced immunity or by the nosocomial catheter, secondary infections could follow it[3-5].

Recently, the frequency of methicillin resistant *S. aureus* (MRSA) emergence gradually has been increased. This bacterium gets the resistance even against vancomycin which was considered as the last treatment antibiotics[6]. Therefore, it has become more important to study the pathogen expression mechanism and develop new antibiotics[7].

Although there is a clinical importance on *S. aureus*, there are not many resolved structures compared to other species. As a part of our structural genomics effort on *S. aureus,* we could characterize a structural information of the SAV2228, translation initiation factor IF-1, belonging to eIF-1a family. The eIF-1a family, which is a member of clan Oligonucleotide/oligosaccharide Binding (OB), includes the eukaryotic translation factor eIF-1A and the bacterial translation initiation factor IF-1.[8] The OB-motif was primally defined by Murzin[9]. The conserved structure of the OB-fold has five-β-sheets to form a closed beta-barrel which is capped by α-helices located between the third and fourth strands.[9]

IF-1 in *S. aureus* Mu50 strain, *infA*, has 72 amino acids which contain OB-fold that can bind to nucleic acid and have calculated pI value of 7.69 and molecular weight of 8.3 kDa. In prokaryotes, initiation of protein biosynthesis starts from the formation of the first peptide bond. Translation initiation requires special components which are consisted of mRNA, fMet-tRNA, initiation factors such as IF-1, IF-2 and IF-3, and at least one GTP molecule.[10] IF-1, as the smallest monomeric protein among three factors, is a highly conserved element of the prokaryotic translational apparatus and could be also found in the chloroplasts of several plants. IF-1 has several functions that primarily are related to translation initiation. First, IF-1 contributes to the enhancement of the rate of 70S ribosome dissociation and subunit association. Second, it stimulates the activity of IF-2 and IF-3 in the formation of the 30S initiation complex. Third, IF-1 binds to the A-site of the 30S ribosomal subunit causing the fidelity of the selection of the mRNA initiation site.

In this paper, we present the sequence-specific resonance assignments and the secondary structure prediction of SAV2228 using TALOS and Chemical Shift Index (CSI) derived from NMR data.

EXPERIMENTAL METHODS

Cloning, expression, and purification The SAV2228 gene was amplified using genomic DNA of *S. aureus* Mu50 and then the PCR product was cloned into a pET-21a vector by using standard cloning protocols. The resulting C-terminal $(His)_6$-tagged protein was expressed in *Escherichia coli* strain

BL21 (DE3) (Novagen) using M9 minimal media supplemented with 1.0 g/*l* [U-^{13}C] glucose and 1.0 g/*l* [^{15}N]NH_4Cl (Cambridge Isotopes Laboratory) as the sole carbon and nitrogen sources respectively. Bacterial cultures were grown at 37 ℃ to an optical density of 0.5-0.6. After 0.5 mM IPTG induction at 37 ℃ for 4 h, the expressed $(His)_6$-tagged protein was then purified with a nickel-chelating column (Qiagen) following the manufacturer's recommendations. Finally, the buffer containing single protein was changed into 20 mM MES, pH 6.0, 50 mM NaCl, 0.1 mM PMSF and 1 mM DTT using dialysis. The purity of the $(His)_6$-tagged protein was estimated to be over 95% by SDS–PAGE. Protein was concentrated up to 1 mM for NMR experiments[11].

NMR experiments 1 mM of ^{13}C, ^{15}N-labled SAV2228 sample was prepared in a final buffer with 90% H_2O/10% D_2O for locking. All NMR experiments were conducted at 303 K on Bruker AVANCE 500 and 600 MHz NMR. A 2D HSQC and a series of triple resonance experiments including 3D HNCACB, 3D HN(CO)CACB, 3D HNCO, 3D HN(CA)CO, 3D HNCA, 3D HN(CO)CA, as well as 3D (H)CCH-TOCSY and 3D ^{15}N-TOCSY-HSQC experiments have been carried out to allow sequence specific backbone and side-chains resonance assignments of the protein. 4,4-dimethyl-4-silapentane-1-sulfonic acid (DSS) was used externally as a chemical shift reference for ^{1}H while ^{13}C and ^{15}N chemical shifts were referenced indirectly using the gyromagnetic ratios of ^{15}N, ^{13}C and ^{1}H (^{15}N/^{1}H = 0.101329118, ^{13}C/^{1}H = 0.251449530)[12]. All NMR spectra were processed with the NMRPipie/nmrDraw[13] and analyzed with the NMRView[14] and SPARKY program. The secondary structure was predicted from the values using CSI[15] and the backbone torsion angles were obtained

using TALOS program[16] which uses a combination of ^{15}N, $^{13}C\alpha$, $^{13}C\beta$, $^{1}H\alpha$ and ^{13}CO chemical shift of triplet of adjacent residues. Besides, we used chemical shift difference method between measured values and random-coil values using Cα, Cβ and (ΔCα- ΔCβ) for predicting secondary structure of SAV2228.

RESULTS AND DISCUSSION

A 2D ^{1}H-^{15}N HSQC spectrum of SAV2228, with assignment indicated, is shown in Fig. 1. The peaks observed in this spectrum are well-dispersed, indicating that the protein is well structured. All expected backbone ^{1}H-^{15}N correlations have been assigned, not including three proline residues (P18, P49 and P59). The first four residues in N-terminus could not be detected. The additional residues, L73 and E74, and hexa-His tag at the C-terminus are also unassigned due to considerable signal overlap. Finally 94.4% of all ^{1}HN, ^{15}N, ^{13}CO, $^{13}C\alpha$ and $^{13}C\beta$ could be assigned. Chemical shifts of ^{1}HN, ^{15}N, ^{13}CO, $^{13}C\alpha$, and $^{13}C\beta$ are presented in Table. 1.

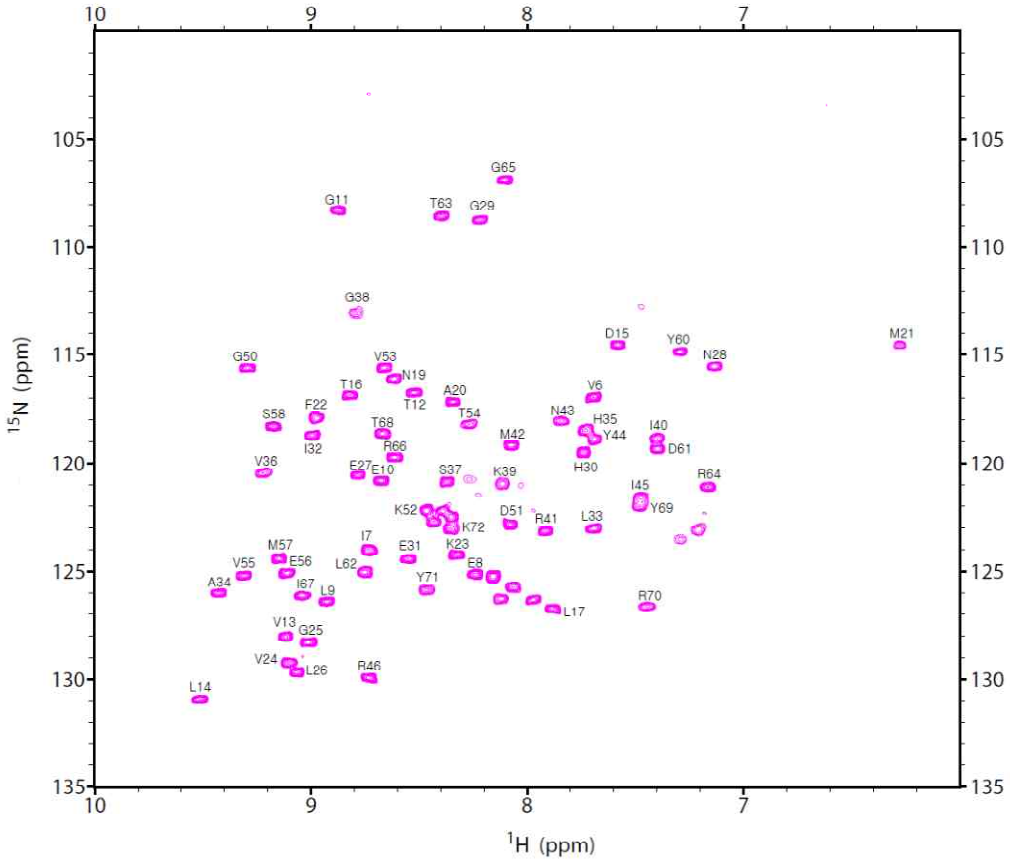

Figure 1. 2D ^{1}HN and ^{15}N HSQC spectrum of SAV2228. The each resonance in the spectrum is labeled with assigned amino acid residues.

Table.1. Chemical shifts of ^{1}HN, ^{15}N, ^{13}CO, ^{13}Cα, and ^{13}Cβ of SAV2228. All chemical shifts were referenced to the frequency of the methyl proton resonances of DSS.

Residue	HN	N	CO	CA	CB	Residue	HN	N	CO	CA	CB
1MET	ND	ND	ND	ND	ND	37SER	8.385	119.773	175.003	57.971	64.767
2ALA	ND	ND	ND	ND	ND	38GLY	8.822	122.166	175.253	46.704	
3LYS	ND	ND	ND	ND	ND	39LYS	8.134	120.001	177.734	58.131	32.640
4GLN	ND	ND	ND	ND	ND	40ILE	7.415	117.821	176.736	61.896	37.830
5ASP	8.368	121.518	175.317	54.861	41.216	41ARG	7.925	122.051	177.543	57.863	29.912
6VAL	7.712	116.000	174.969	60.966	34.891	42MET	8.099	118.145	175.862	56.459	32.266
7ILE	8.755	123.005	174.177	60.278	40.778	43ASN	7.856	117.041	174.616	53.663	38.812

8GLU	8.254	124.217	175.592	54.713	32.478	44TYR	7.713	117.847	175.211	58.654	37.617
9LEU	8.953	125.396	174.654	53.767	47.167	45ILE	7.481	120.624	173.895	61.280	38.081
10GLU	8.705	119.838	176.424	55.255	31.636	46ARG	8.089	124.838	174.759	55.534	30.762
11GLY	8.898	107.237	171.493	45.656		47ILE	7.981	125.340	173.922	60.898	37.641
12THR	8.551	115.748	174.347	61.293	71.247	48LEU	8.759	128.936	174.217	51.630	43.514
13VAL	9.139	127.055	175.760	64.720	31.470	49PRO			176.960	64.033	31,011
14LEU	9.539	129.919	176.277	55.675	43.905	50GLY	9.321	114.565	174.448	44.654	
15ASP	7.605	113.571	174.864	53.257	44.745	51ASP	8.100	121.866	175.327	55.393	41.197
16THR	8.840	115.833	172.704	60.289	69.414	52LYS	8.425	121.338	176.315	54.637	32.499
17LEU	7.909	125.704	174.509	52.925	42.504	53VAL	8.686	114.744	174.278	57.956	36.138
18PRO			175.973	63.166	32.222	54THR	8.305	117.278	173.923	62.437	69.902
19ASN	8.624	115.160	174.180	54.137	36.851	55VAL	9.336	124.180	174.106	59.542	34.494
20ALA	8.351	116.145	174.990	52.903	16.490	56GLU	9.131	124.031	176.645	54.351	32.598
21MET	6.294	113.547	175.205	53.179	35.025	57MET	9.163	123.444	174.899	54.266	36.117
22PHE	9.010	116.878	174.697	57.166	43.136	58SER	9.198	117.358	174.693	54.727	64.521
23LYS	8.340	123.155	175.853	55.594	33.905	59PRO			176.290	63.919	31.573
24VAL	9.124	128.269	173.199	60.705	35.562	60TYR	7.317	113.864	175.439	57.391	39.988
25GLU	9.025	127.357	176.358	54.907	31.457	61ASP	7.417	118.358	174.996	53.842	41.326
26LEU	9.108	128.629	179.339	54.822	43.494	62LEU	8.763	124.066	177.109	55.172	40.855
27GLU	8.802	119.552	175.724	58.422	29.525	63THR	8.418	107.622	174.873	62.721	70.339
28ASN	7.175	114.579	176.299	52.481	37.610	64ARG	7.192	120.109	174.858	54.212	34.514
29GLY	8.252	107.824	174.243	45.206		65GLY	8.139	105.977	171.075	45.282	
30HIS	7.750	118.973	173.476	55.265	29.991	66ARG	8.620	118.614	175.345	53.681	33.272
31GLU	8.512	123.476	176.181	55.116	31.680	67ILE	9.089	125.192	176.084	61.927	39.242
32ILE	9.008	117.654	174.438	59.190	43.081	68THR	8.694	117.586	174.406	61.334	69.509
33LEU	7.712	122.059	176.190	53.773	43.666	69TYR	7.494	120.983	172.657	58.734	41.279
34ALA	9.450	125.041	175.700	50.216	23.017	70ARG	7.450	125.725	174.016	54.661	31.543
35HIS	7.74	117.615	174.787	54.391	33.073	71TYR	8.483	124.947	175.278	58.440	38.662
36VAL	9.233	119.182	175.551	62.294	33.33	72LYS	8.363	122.047	176.160	56.046	33.309

*ND; Not Detected **Unit; ppm

Secondary structural information was obtained on the basis of chemical shifts. The chemical shift is a good means of a sensitive measure of molecular conformation, backbone dihedral angle, hydrogen bond interactions, backbone dynamics and ring-flip rates. We used two programs to get secondary structure information. One is CSI. Analysis of the $^{1}H\alpha$, $^{13}C\alpha$, $^{13}C\beta$ and ^{13}CO chemical shift using CSI has become a standard method for predicting secondary structure of protein by characterizing deviation of chemical shifts of certain nuclei in amino acid relative to their random coil values[15]. The other one, TALOS program, was also used to get backbone dihedral angles (φ, ψ) information using chemical shift values[16]. Analysis of the chemical shift difference of $^{13}C\alpha$ and $^{13}C\beta$ difference between measured values and ramdom-coil values agree with results of CSI and TALOS

program. The analysis of backbone resonance assignment of SAV2228 is summarized in Fig. 2. As shown in Fig. 2, examination of (ΔCα- ΔCβ) plot shows the possible presence of one α-helix and five β-sheets. The region of α-helix and β-sheets corresponds to the results of the CSI and TALOS. The predicted secondary structure of SAV2228 is largely consistent with the conserved structure of the OB-fold, a five-stranded beta-sheet to form a closed beta-barrel[9].

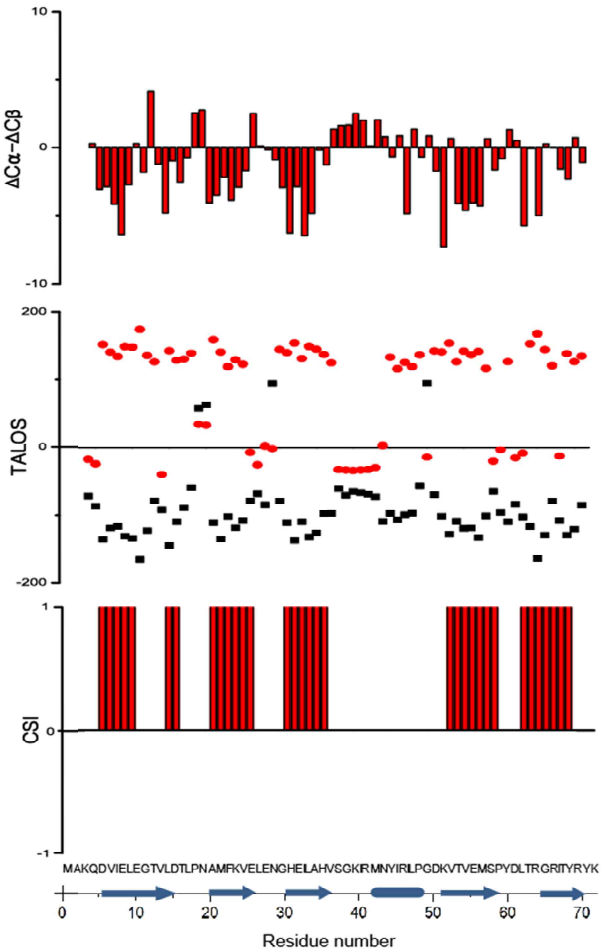

Figure 2. Summary of backbone resonance assignment of SAV2228. Delta values (ΔCα- ΔCβ) of backbone carbon to random coil chemical shifts were plotted. In the consensus CSI, the values '-1'

represents the α-helical tendency while '1' represents the β-strand. Backbone dihedral angles were calculated using TALOS. Filled rectangles and circles indicated the predicted phi and psi angles respectively. Predicted secondary structure elements of SAV2228 were shown in box for α-helix and arrows for β-strand.

There are several pre-identified structures of bacterial IF-1[10,17], archaea IF-1[18], and eukaryotic IF-1[19,20]. SAV2228 belongs to bacteria and has similar secondary structure with other species. They consist of β-β-β-α-β-β tructure, but the specific residues and the length of secondary structures were not completely same. Eukaryotic IF-1 has the different number of amino acids. So it has additional two α-helices following bacterial secondary structure.

SAV2228 (IF-1) adopts the expected OB fold, which interacts with oligonucleotide/oligosaccharide. In further study, NMR titration experiment can be used to verify exact nucleic acid binding site in SAV2228.

Acknowledgements

This study was supported by a National Research Foundation of Korea (NRF) grant funded by the Korean government (MEST) (Grant number 2012R1A2A1A01003569 & 20110001207). This study was also supported by a grant from the Korea Healthcare technology R&D Project, Ministry for Health, Welfare & Family Affairs, Republic of Korea (Grant number: A092006). This work was supported in part by the 2011 BK21 project for Medicine, Dentistry, and Pharmacy. We thank

National Center for Inter-University Research Facilities (NCIRF) for using their NMR machines .

REFERENCES

1. P. Bhateja, K. Purnapatre, S. Dube, T. Fatma, A. Rattan, *Int. J. Antimicro. Ag.* **27**, 201 (2006).
2. K. Shimada *et al.*, *Jpn. J. Antibiot.* **54**, 331 (2001).
3. Z. A. Mirani, N. Jamil. *JCPSP* **20**, 558 (2010).
4. P. D. Mauldin, C. D. Salgado, V. L. Durkalski, J. A. Bosso, *Annals Pharmacother.* **42**, 317 (2008).
5. M. W. Pletz, O. Burkhardt, T. Welte, *Eur. J. Med. Res.* **15**, 507 (2010).
6. K. Hiramatsu, L. Cui, M. Kuroda, T. Ito, *Trends Microbiol.* **9**, 486 (2001).
7. F. C. Tenover, J. W. Biddle, M. V. Lancaster, *Emerg. Infect. Diseases* **7**, 327 (2001).
8. N. C. Kyrpides, C. R. Woese, *Proc. Natl. Acad. Sci. U S A* **95**, 224 (1998).
9. A. G. Murzin, *EMBO J.* **12**, 861 (1993).
10. M. Sette *et al.*, *EMBO J.* **16**, 1436 (1997).
11. S.-B. Jang, C. Ma, P. C. Chandan, D.-H. Kim, B.-J. Lee, *JKMRS* **15**, 69 (2011).
12. S.-B. Jang, C. Ma, S. J. Park, A.-R. Kwon, B.-J. Lee, *JKMRS* **13**, 117 (2009).
13. F. Delaglio *et al.*. *J. biomol. NMR* **6**, 277 (1995).
14. B. A. Johnson, *Methods Mol. Biol.* **278**, 313 (2004).
15. D. S. Wishart, B. D. Sykes, *J. biomol. NMR* **4**, 171 (1994).
16. G. Cornilescu, F. Delaglio, A. Bax, *J. biomol. NMR* **13**, 289 (1999).
17. G. N. Hatzopoulos, J. Mueller-Dieckmann, *FEBS lett.* **584**, 1011 (2010).
18. W. Li, D. W. Hoffman, *Prot. Sci.* **10**, 2426 (2001).
19. C. M. Fletcher, T. V. Pestova, C. U. Hellen, G. Wagner, *EMBO J* **18**, 2631 (1999).
20. J. L. Battiste, T. V. Pestova, C. U. Hellen, G. Wagner, *Mol cell* **5**, 109 (2000).